

## A New Strategy for Ratiometric Fluorescence Detection of Transition Metal Ions

Sandip Banthia and Anunay Samanta\*

*School of Chemistry, University of Hyderabad, Hyderabad - 500 046, India*

*Received: February 6, 2006; In Final Form: March 3, 2006*

A novel design strategy for ratiometric fluorescence signaling of transition metal ions, involving both photoinduced electron transfer and resonance energy transfer mechanisms, has been tested on a model system comprising dual fluorophores.

Fluorescent systems, which are capable of sensing various chemically, environmentally, and biologically significant species, are of great current interest.<sup>1</sup> A majority of these fluorescent sensors are three-component systems comprising a signaling unit, a guest binding unit, and a linker that connects these two units. The signaling unit, called fluorophore, is responsible for the absorption and emission of light, the guest binding unit, called receptor, is essential for the complexation and de-complexation of the guest, and the linking unit, called spacer, often plays a key role in establishing the electronic communication between the fluorophore and receptor. Compared to the large number of fluorophore–spacer–receptor systems available for sensing alkali and alkaline earth metal ions, only few fluorescent sensor systems for the transition metal ions are described in the literature.<sup>2–4</sup> Most of the reported transition metal ion sensors exhibit quenching of fluorescence in the presence of the metal ions, and only a few systems are known that exhibit enhancement of fluorescence.<sup>5–9</sup> However, since several factors, such as phototransformation, sensor concentration, and environmental effects,<sup>10</sup> contribute to fluorescence intensity modulation of a system, ratiometric fluorescence signaling, which involves measurement of the changes in the ratio of the fluorescence intensities at two different wavelengths,<sup>11</sup> is preferred to the conventional method of monitoring the fluorescence intensity at a single wavelength. In this respect, we note that, among the large number of available fluorescent sensors, only a few systems that offer ratiometric response are reported, with practically none for the transition metal ions.<sup>12–19</sup>

The major challenge to ratiometric fluorescence signaling is to develop a system with two emitting states having both wavelength- and substrate-dependent emission properties. Exciplex or excimer emission has often been exploited for ratiometric signaling of alkali metal ions.<sup>18,19</sup> Taking into consideration the fact that systems having a fluorophore<sub>1</sub>–spacer–fluorophore<sub>2</sub> architecture with properly chosen components can show resonance energy transfer (RET) from the donor fluorophore to the acceptor fluorophore and hence can exhibit emission at two different wavelengths,<sup>20</sup> we thought that it might be possible to accomplish the task of ratiometric signaling of transition metal ions by incorporating a photoinduced electron transfer (PET) signaling mechanism into this

system. Conceptually, this leads to system having a branched fluorophore<sub>1</sub>–spacer(spacer-receptor)–fluorophore<sub>2</sub> or linear fluorophore<sub>1</sub>–spacer<sub>1</sub>–fluorophore<sub>2</sub>–spacer<sub>2</sub>–receptor architecture. Herein, this novel design strategy of ratiometric fluorescence signaling of transition metal ions has been tested on a simple model system (**1**) having a fluorophore<sub>1</sub>–spacer-(spacer-receptor)–fluorophore<sub>2</sub> architecture (Figure 1). We note in this context that de Silva and co-workers have previously developed linear systems with a fluorophore<sub>1</sub>–spacer<sub>1</sub>–receptor–spacer<sub>2</sub>–fluorophore<sub>2</sub> format for ratiometric pH signaling purpose.<sup>21</sup> These systems, termed as second generation fluorescent sensors, are actually linear extension of the fluorophore–spacer–receptor architecture and built by derivatization of the terminal receptor moiety. In these systems, the second fluorophore, which is nonresponsive to the guest, is used for referencing the fluorescence level of the first fluorophore and the energy transfer between the two fluorophores is incidental. On the other hand, in our fluorophore<sub>1</sub>–spacer(spacer-receptor)–fluorophore<sub>2</sub> system, which is conceived from the fluorophore<sub>1</sub>–spacer–fluorophore<sub>2</sub> format and the receptor moiety, the energy transfer process between the two terminal fluorophores forms the heart of the design strategy, and the receptor unit is branched out of the fluorophore<sub>1</sub>–spacer–fluorophore<sub>2</sub> chain.

In our dual-fluorophore system, which is the first of its kind, we have employed a simple aliphatic amino functionality as the receptor for the transition metal ions and also for communication with the fluorophores via PET mechanism.<sup>22</sup> Anthracene and 4-amino-7-nitrobenzoxa[1,3]diazole (ANBD) moieties have been chosen as the fluorophore components because of their distinct absorption and emission features; in particular, the overlap of the fluorescence and absorption spectra of anthracene and ANBD, respectively, a feature essential for RET between these fluorophore moieties.<sup>20</sup>

Compound **1** has been synthesized by following a two-step synthetic procedure. The first step involved preparation of **2** by condensation of 9-anthranaldehyde with *N,N*-dimethylethylenediamine followed by reduction of the schiff base formed with sodium borohydride.<sup>23</sup> In the second step, **2** was reacted with 4-chloro-7-nitrobenzoxa[1,3]diazole to obtain the desired dual-fluorophore system. The absorption and fluorescence spectra were recorded on Shimadzu UV-3101PC spectrophotometer and Spex Fluoromax-3 spectrofluorimeter, respectively.

\* Corresponding author. E-mail: assc@uohyd.ernet.in

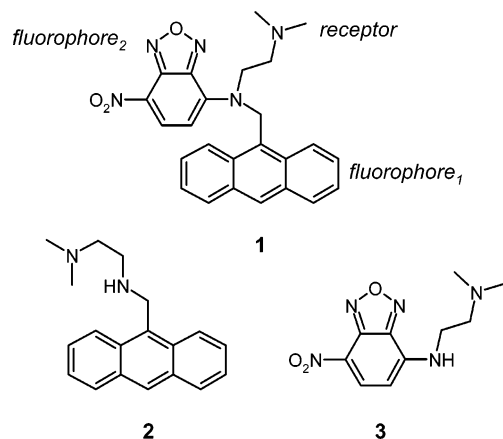


Figure 1. Molecular structures of **1**, **2**, and **3**.

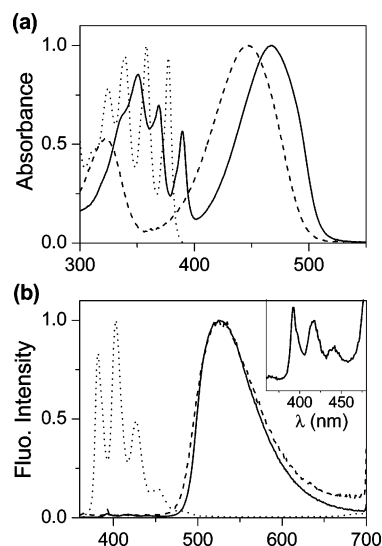


Figure 2. Absorption (a) and fluorescence (b) spectra of **1** (solid line), ANBD (dashed line), and anthracene (dotted line), normalized at their respective peak positions, in THF. Inset: short wavelength region of the emission of **1** in an expanded scale. Excitation wavelength = 350 nm.

The fluorescence decay curves were measured on a single photon-counting nano-LED spectrofluorimeter (IBH).

The electronic absorption spectrum of **1** in tetrahydrofuran (THF) is characterized by a broad band centered at 468 nm and a structured band between 310 and 400 nm (Figure 2a). While the structured band, which is insensitive to the solvent polarity, is characteristic of the anthracene chromophore, the long wavelength band, which exhibits Stokes shift with increase in the polarity of the medium, is typical of the intramolecular charge transfer (ICT) transition in the ANBD fluorophore.<sup>24</sup>

Compound **1** exhibits two-component fluorescence, the exact nature of which is dependent on the excitation wavelength. When excited at  $\sim 440$  nm, where the absorption is exclusively due to the ANBD moiety, an intense broad emission band (centered around 528 nm in THF) typical of the ANBD moiety is observed. However, when excited at  $\sim 350$  nm, where the absorption is predominantly due to the anthracene moiety (see Figure 2a), the emission spectrum consists of a very weak anthracene-like structured band between 380 and 460 nm along with the highly intense long-wavelength broad band due to the ANBD moiety (Figure 2b). The fluorescence quantum yield ( $\varphi_f$ ) due to the ANBD moiety, which can be determined accurately because of noninterference due to the anthracene chromophore at the excitation wavelength, 440 nm, is measured to be 0.46

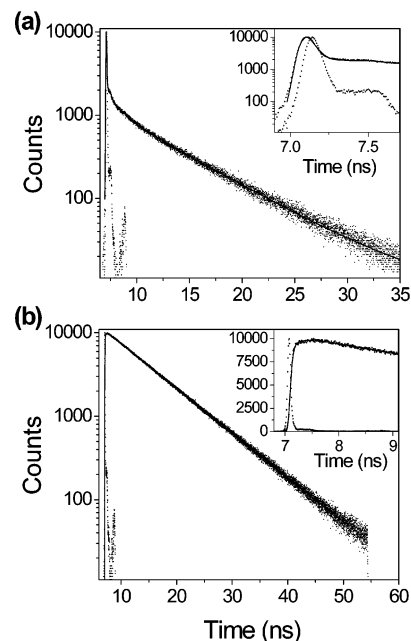
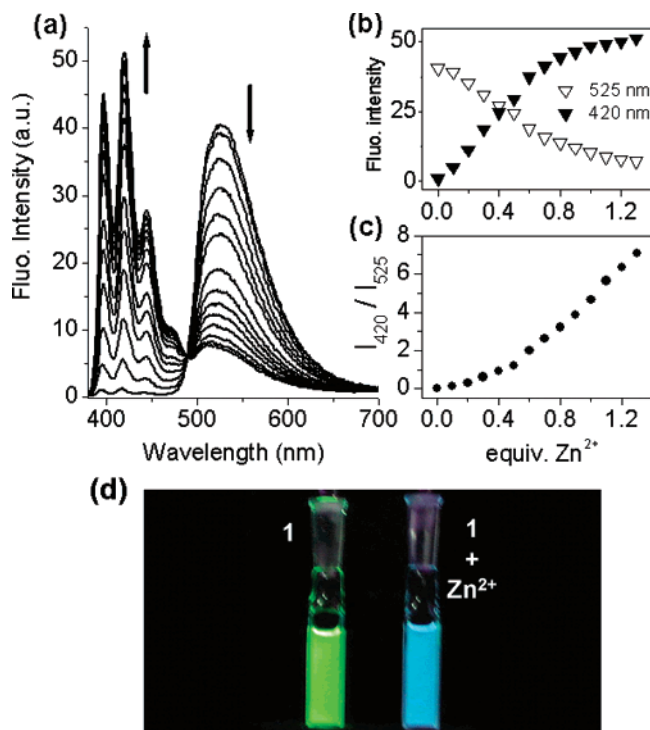


Figure 3. Fluorescence decay profiles ( $\lambda_{\text{exc}} = 374$  nm) of **1** in THF at 425 nm (a) and 550 nm (b). The insets show the short-time behavior of the decay profiles more clearly. The decay parameters for the fits shown in the figure are (a)  $\tau_1 = 0.031$  ns (0.95),  $\tau_2 = 6.1$  ns (0.028),  $\tau_3 = 1.0$  ns (0.022); and (b)  $\tau_1 = 8.1$  ns,  $\tau_2 = 0.035$  ns ( $-0.89$ ),  $\tau_3 = 0.35$  ns ( $-0.11$ ).

in THF. A slightly lower  $\varphi_f$  value of **1** compared to the parent fluorophore ANBD ( $\varphi_f = 0.9$  in THF)<sup>24</sup> can be due to the possible PET interaction between the receptor and ANBD moieties. On the other hand,  $\varphi_f$  of **1** corresponding to the short-wavelength structured emission is measured to be only 0.0023 in THF. This value is drastically lower than the  $\varphi_f$  value of the bare fluorophore, anthracene ( $\varphi_f = 0.297$  in THF).<sup>23</sup> Nearly 130-fold lower fluorescence efficiency of **1** compared to anthracene can be attributed to the combined effect of PET between the receptor and the anthracene moiety and RET from the anthracene moiety to the ANBD moiety of the system.

The fluorescence decay behavior of **1** has been studied carefully with a view to obtain conclusive evidence in favor of the PET and RET processes in the system. The fluorescence time profile at 425 nm, where only the emission due to the anthracene moiety contributes, consists of a major component (95%) with the lifetime ( $\tau_f$ ) of 0.031 ns (Figure 3a), which is significantly shorter than that of anthracene (3.8 ns). Two other minor components with lifetimes 6.1 ns (2.8%) and 1.0 ns (2.2%) are also observed. In this context it is to be noted that our attempts to fit to the decay profile with a single/biexponential function or to a distribution of lifetimes (employing a second exponential component in the fitting function) yielded residuals and  $\chi^2$  values that were unacceptable. While the minor component with lifetime of 1.0 ns can arise from a small number of molecules in which the anthracene moiety experiences a less quenching environment because of a different spatial disposition of the quenching receptor moiety, we are unable to comment on the possible origin of the other minor component whose lifetime is larger than that of anthracene. On the other hand, a triexponential fit to the fluorescence decay profile at 550 nm was found the most satisfactory. This fit yielded two components with negative preexponential factors and one with positive preexponential factor. The component with positive preexponential factor has a lifetime of 8.1 ns, which is slightly lower than the lifetime of ANBD (11.5 ns). The major negative



**Figure 4.** (a) Fluorescence spectra of **1** (10<sup>-5</sup> M in THF,  $\lambda_{exc}$  = 370 nm) upon titration with Zn<sup>2+</sup> ions. (b) Titration profiles at 420 and 525 nm. (c) Intensity ratio of fluorescence at 420 nm to that at 525 nm vs equivalents of Zn<sup>2+</sup> ions. (d) Fluorescence of **1** before and after addition of Zn<sup>2+</sup> ions (samples were excited at 365 nm using UV lamp).

component (89%) associated with a lifetime of 0.035 ns is almost identical with that of the anthracene-like emission monitored at 425 nm. Therefore, the growing component at 550 nm clearly arises due to RET from anthracene to the ANBD moiety. At this stage, we are unable to comment on what contributes to the second growing component. It should be noted that the time-profile of the fluorescence at 550 nm, when measured on excitation of the sample at 439 nm, is represented by a single exponential decay with a lifetime of 8.1 ns (see Supporting Information).

The fluorescence signaling ability of **1** has been examined for several alkali, alkaline earth, transition, and heavy metal salts. In the presence of alkali and alkaline earth metal ions, **1** does not show any spectral change. However, addition of transition metal salts leads to an enhancement of the emission intensity in the short-wavelength region and simultaneous decrease of the long-wavelength emission intensity of **1** thus providing a wavelength ratiometric response to transition metal ions. Typical changes in the emission spectra of **1** are shown in Figure 4. A clear isosbestic point in the emission spectra suggests that two distinct species are present at the equilibrium. The titration profiles shown in Figure 4b correspond to 1:1 stoichiometry, though a “two-step linear” correlation between the ratio of fluorescence at 420 nm to those at 525 nm and metal ion concentration has been observed (Figure 4c).

The results, a decrease of the fluorescence due to the ANBD moiety and an increase of the emission due to the anthracene moiety, can be explained only if the binding of the metal ions with the amine receptor results in inhibition of (i) the PET communication between the receptor nitrogen atom and the anthracene fluorophore and (ii) the RET process between the two fluorophore moieties. Thus, the signal transduction mechanism employed here makes the present system unique compared to other sensing schemes. Moreover, unlike other sensing

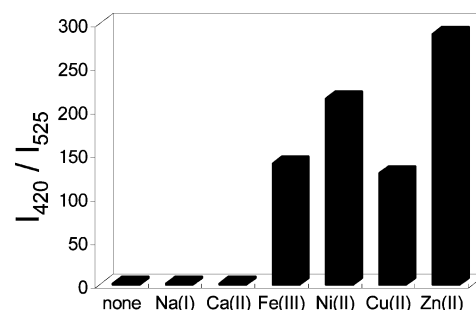


**Figure 5.** Fluorescence ratiometric response of **1** to selected metal ions in THF: change in the ratio of fluorescence intensity at 420 nm to that at 525 nm for different metal ions. The response is normalized with respect to the fluorescence intensity ratio of “free” **1**. Excitation wavelength = 370 nm.

schemes, where either the initial or the final state is fluorescent, here both the situations are strongly fluorescent. While the analyte-free state displays strong green fluorescence due to the emission from the CT state of the ANBD fluorophore, the analyte-bound state comprising anthracene-like emission displays strong blue fluorescence (Figure 4d). It should be noted that in the presence of transition metal ions other than Zn<sup>2+</sup>, the enhancement of the anthracene-like emission is relatively less, while the quenching of the ANBD-like emission is similar to that observed in the presence of Zn<sup>2+</sup> ions (see Supporting Information). The internal quenching of the anthracene fluorophore in the presence of transition metal ions such as Cu(II) is presumably due to energy transfer with the metal's d–d manifold acting as energy acceptor. The effect of the metal ions on the fluorescence decay behavior has also been studied. In the presence of transition metal ions, the subnanosecond component of the fluorescence decay disappears completely and a significant increase in the amplitude of the long component is observed on progressive addition of the transition metal salts (see Supporting Information). For instance, the decay parameters for **1** observed at 425 nm in the presence of one equivalent of Zn<sup>2+</sup> are 8.2 ns (96%) and 1.1 ns (4%) in THF. An increase in the average lifetime of **1** in the presence of the metal ions is clearly due to the metal ion-induced suppression of PET and RET in the multicomponent system.

The signaling response of **1** can be compared with that of simple PET-based fluorophore–spacer–receptor systems, **2** and **3**, which comprise either anthracene or ANBD fluorophore. Structure **2** acts as a “turn-on” sensor only in the presence of Zn<sup>2+</sup> ions.<sup>23</sup> Other transition metal ions do not show “off–on” signaling response because of their quenching influence<sup>25,26</sup> on the anthracene chromophore. The fluorescence of **3**, though it switches “on” even in the presence of quenching paramagnetic metal ions due to the inhibition of very efficient PET in the system,<sup>24</sup> does not afford ratiometric signaling. In **1**, there is no significant PET between the receptor and the ANBD moiety and hence, addition of the transition metal ions results in quenching of ANBD emission, thus allowing to monitor the changes ratiometrically (Figure 5).

In summary, the fluorescence response of a multicomponent model system, designed with a view to testing a new strategy for ratiometric signaling of transition metal ions, has been studied. The results clearly point to the effectiveness of the design strategy and suggest that it would be possible to develop sensor systems for practical usage based on the present design principle when the fluorophore and receptor components are chosen such that the signaling studies can be carried out in aqueous media. Work in this direction is currently underway. We are also in the process of engineering this design with

receptors suitable for the specific binding, particularly in water, which may lead to ratiometric fluorescent probes for selective detection of the given analyte.

**Acknowledgment.** This work is supported by the Department of Science and Technology (DST), Government of India; Council of Scientific and Industrial Research (CSIR) and UPE Program of the University Grants Commission (UGC). S.B. thanks CSIR for the Fellowship.

**Supporting Information Available:** Experimental details, spectral data, additional absorption and fluorescence spectra and fluorescence decay profile. This material is available free of charge via the Internet at <http://pubs.acs.org>.

## References and Notes

- (1) de Silva, A. P.; Tecilla, P. Special Issue on Fluorescent Sensors; *J. Mater. Chem.* **2005**, *15*.
- (2) de Silva, A. P.; Gunaratne, H. Q. N.; Gunnlaugsson, T.; Huxley, A. J. M.; McCoy, C. P.; Rademacher, J. T.; Rice, T. E. *Chem. Rev.* **1997**, *97*, 1515.
- (3) Fabbri, L. Special Issue on Luminiscent Sensors, *Coord. Chem. Rev.* **2000**, *205*.
- (4) Rurack, K. *Spectrochim. Acta, Part A* **2001**, *57*, 2161.
- (5) Ghosh, P.; Bharadwaj, P. K.; Mandal, S.; Ghosh, S. *J. Am. Chem. Soc.* **1996**, *118*, 1553.
- (6) Ramachandram, B.; Samanta, A. *Chem. Commun.* **1997**, 1037.
- (7) Rurack, K.; Kollmannsberger, M.; Resch-Genger, U.; Daub, J. *J. Am. Chem. Soc.* **2000**, *122*, 968.
- (8) Banthia, S.; Samanta, A. *J. Phys. Chem. B* **2002**, *106*, 5572.
- (9) Banthia, S.; Samanta, A. *Org. Biomol. Chem.* **2005**, *3*, 1428.
- (10) Lakowicz, J. R. *Topics in Fluorescence Spectroscopy*; Plenum Press: New York, 1994; Vol. 4.
- (11) Grynkiewicz, G.; Poenie, M.; Tsien, R. Y. *J. Biol. Chem.* **1985**, *260*, 3440.
- (12) Mohr, G. J.; Klimant, I.; Spichiger-Keller, U. E.; Wolfbeis, O. S. *Anal. Chem.* **2001**, *73*, 1053.
- (13) Mello, J. V.; Finney, N. S. *Angew. Chem., Int. Ed.* **2001**, *40*, 1536.
- (14) Maruyama, S.; Kikuchi, K.; Hirano, T.; Urano, Y.; Nagano, T. *J. Am. Chem. Soc.* **2002**, *124*, 10650.
- (15) Burdette, S. C.; Lippard, S. *Inorg. Chem.* **2002**, *41*, 6816.
- (16) Yang, R.; Li, K.; Wang, K.; Zhao, F.; Li, N.; Liu, F. *Anal. Chem.* **2003**, *75*, 612.
- (17) Taki, M.; Wolford, J. L.; O'Halloran, T. V. *J. Am. Chem. Soc.* **2004**, *126*, 712.
- (18) Nishizawa, N.; Watanabe, M.; Uchida, T.; Teramae, N. *J. Chem. Soc., Perkin Trans. 2* **1999**, 141.
- (19) Sankaran, N. B.; Nishizawa, S.; Watanabe, M.; Uchida, T.; Teramae, N. *J. Mater. Chem.* **2005**, *15*, 2755.
- (20) Lakowicz, J. R. *Principles of Fluorescence Spectroscopy*, 2nd ed.; Kluwer Academic/Plenum Publishers: New York, 1999.
- (21) de Silva, A. P.; Gunaratne, H. Q. N.; Gunnlaugsson, T.; Lynch, P. L. *M. New J. Chem.* **1996**, *20*, 871.
- (22) Bissel, R. A.; de Silva, A. P.; Gunaratne, H. Q. N.; Lynch, P. L. M.; Maguire, G. E. M.; McCoy, C. P.; Sandanayake, K. R. A. S. *Top. Curr. Chem.* **1993**, *168*, 223.
- (23) Bag, B.; Bharadwaj, P. K. *J. Phys. Chem. B* **2005**, *109*, 4377.
- (24) Ramachandram, B.; Samanta, A. *J. Phys. Chem. A* **1998**, *102*, 10579.
- (25) Varnes, A. W.; Dodson, R. B.; Wehry, E. L. *J. Am. Chem. Soc.* **1972**, *94*, 946.
- (26) Kemlo, J. A.; Shepherd, T. M. *Chem. Phys. Lett.* **1977**, *47*, 158.